Dynamic testing of a helicopter landing pad: comparison between operational and experimental approach

Giorgio Busca · Alfredo Cigada · Elena Mola · Franco Mola · Marcello Vanali

Received: 4 July 2013 / Revised: 3 October 2013 / Accepted: 11 November 2013 / Published online: 28 November 2013

1 Introduction

Nowadays, when a new edifice is built, it is a common rule in Italy and in other countries to execute both static and dynamic tests on the structure. Moreover, if the building or structure is considered strategic according to the Italian construction code, a full-scale dynamic testing is required. In this way, it is not only possible to validate the design, conformingly with anti-seismic requirements, but also to estimate the dynamic parameters that will be used as a reference for future structural health-monitoring activities based on dynamic measurements [1–3]. Dynamic testing against seismic requirements becomes crucial and compulsory according to Italian laws when a building or one of its parts is considered strategic in case of an emergency. This is especially true with regard to the Palazzo Lombardia building complex that is the new seat for the regional government and its integrity must be ensured even in case of earthquakes and other catastrophic events.

Among the complex parts, the helicopter landing pad is a crucial element of the buildings where the "Regione Lombardia" headquarter is based; for this reason, it needs to be tested to guarantee its safety under all conditions. As it will be shown in the Sect. 2, the structure under test has peculiar characteristics such as radial symmetry and the multidirectional joints, which allow the structure to move both in the vertical and horizontal directions. These characteristics are difficult to model and therefore experimental data are required to tune and update the FEM model developed by the designer. Moreover, the Italian and

G. Busca (✉) · A. Cigada
Mechanical Engineer Department, Politecnico di Milano, Via La Masa 1, Milan, Italy
e-mail: giorgio.busca@polimi.it

E. Mola
ECSD S.r.l, Via Goldoni, Milan, Italy

F. Mola
Department of Architecture, Built Environment and Construction Engineering, Politecnico di Milano, Piazza Leonardo da Vinci 32, Milan, Italy

M. Vanali
Industrial Engineer Department, Università di Parma, Viale G.P. Usberti 181/A, Parma, Italy

European standards suggest performing both static and dynamic tests during the acceptance procedure, to validate the numerical models on the dynamic behavior, making them a valid tool to assess the structural reliability during earthquakes. Modal analysis is not only needed to fix the starting picture of the structure (modal parameters at the structure birth), but it is also one of the most popular ways to perform health monitoring during structure life. Among the several health-assessing methods available in literature, the vibration-based damage identification technique seems to be one of the most promising. Civil infrastructure integrity can be evaluated by extracting information from the dynamic response measurements. The basic idea is that damage induces changes in the physical properties and consequently detectable changes in modal properties. For these reasons, modal parameters are some of the most used indicators in literature to represent the behavior of the structure and therefore to assess the health status [4–6].

Modal parameter estimation can be performed by two different approaches: applying a known excitation (by means of a hydraulic actuator, vibrodyne, etc.) or exploiting the unknown loading caused by environment load sources (such as traffic, wind, etc.). The first is called experimental modal analysis (EMA), whereas the second is known as operational modal analysis (OMA) [7–9]. As it is not possible to impose continuously an excitation to a civil structure during its normal life, OMA tests are preferable to ensure safe monitoring. However, EMA tests give results that are more accurate and are thus useful to define the reference step. Therefore, they are normally carried out, once a structure is built, to provide the initial "picture" of the structure status. EMA guarantees generally a total control on the test conditions: the excitation level may be fixed for every analysis and the results, obtained with different forcing amplitudes, can be compared with each other. Moreover, it is possible to keep a detailed record of all the external influencing parameters, such as temperature and humidity. Nevertheless, EMA is expensive and time consuming, a proper actuator has to be placed on the structure and measurements cannot be recorded continuously [10, 11].

On the other hand, OMA does not have the same control on the influencing parameters, as some of them are not even measurable [12, 13]. In this case, the excitation input of the system is not known, and only some assumptions can be made. Moreover, these assumptions can be misleading, since the excitation input is due to sources such as traffic, wind or people walking on the structure. Huth et al. [14] show the advantages of using output-only system identification, but the results stress how the modal parameter estimation is deeply affected by the environment conditions. Indeed, the challenge of today's research is the definition of damage identification features independent of

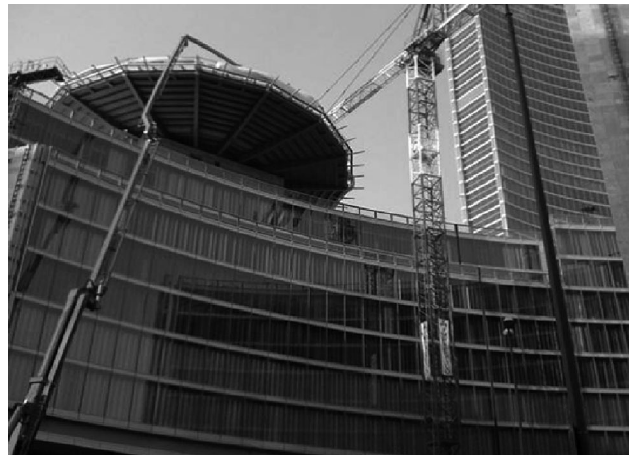

Fig. 1 Helisurface

humidity, temperature, etc. However, this method is cheaper and easier to carry out. The only needs are a proper number of transducers placed on the structure and a continuous data acquisition system [15]. By exploiting this setup, a continuous monitoring of the modal parameters can be performed [13]. These advantages make operational modal analysis suitable for a continuous monitoring of the structure status and damage identification.

This paper deals with the comparison of the two abovementioned modal analysis methods applied to a real case: *Palazzo della Regione* helisurface, built in Milano in 2010. EMA and OMA techniques are applied to define the dynamic behavior in the range 0–10 Hz, which is a typical bandwidth of interest for civil structure. At first, a description of the structure is proposed, and then the chosen measurement setup is defined and justified. In the end, the obtained results are compared and discussed.

It must be noticed that OMA results are strengthened by a direct comparison to the EMA ones, providing an experimental assessment of their reliability and setting the basis for assessing the structural behavior evolution. A good agreement between EMA and OMA is required to guarantee that the constraints, at the base of the operational approach, are satisfied by the tested structure (and its environment) and to identify possible disturbances that will lead to erroneous mode identifications [13]. Particular attention will be paid to the OMA results in terms of reliability of the identified parameters for their application to the structural health monitoring of the specific structure.

2 Structure

The mentioned helisurface has a circular layout and is placed on the top of elevators and services group, called core 4, of "Altra Sede della Regione Lombardia", as shown in Fig. 1. The structure is composed of a landing

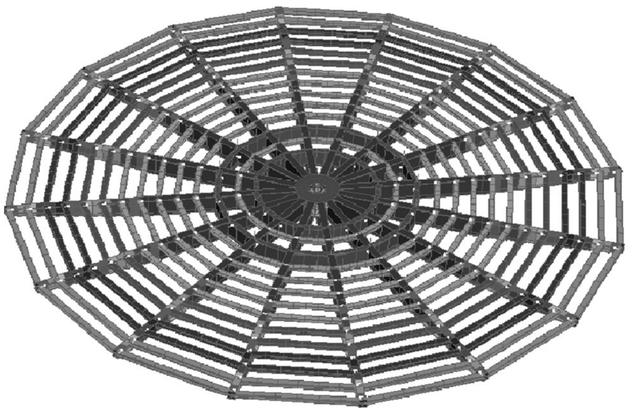

Fig. 2 Beam structure of the helisurface

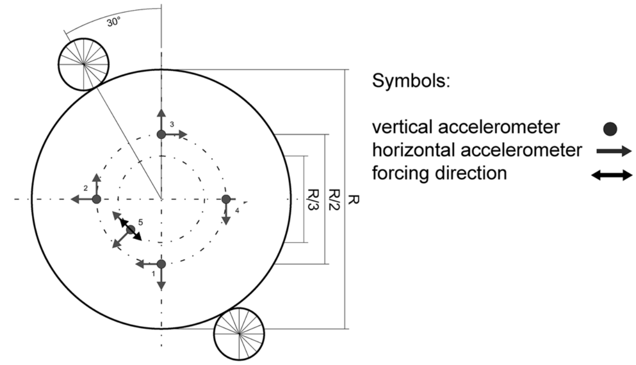

Fig. 3 Sensor placement for the horizontal direction

circular plane (34 m diameter), surrounded by a protection grid (2 m tall) along the perimeter. The access to the structure is possible by means of two metallic helicoidal stairs.

The main structure is composed of 16 double T beams (variable height from 130 cm to 40 cm) constructed in radial symmetry with a 22.5 degree angle among them. These beams are connected to each other through secondary elements, which form concentric polygonal rings with wheelbase of about 1 m.

The deck is obtained with a 21 cm depth reinforced concrete slab. The radial beams are connected to the slab by means of bolted joints. The structure supports are made of reinforced neoprene material, with a thickness of 47 mm. These supports, thanks to their deformability, allow the thermal deformation of the structure, minimizing the solicitations. Moreover, they represent a multidirectional joint for the horizontal solicitations. The constraints are positioned in correspondence to the two inner violet circles in Fig. 2. The seismic behavior of the helisurface is completely unrelated to the supporting structure.

Because of the neoprene joints, both horizontal and vertical modes are needed to fully describe the helisurface behavior and they will be analyzed exploiting the experimental setup described in the next paragraph.

3 Experimental setup

This section describes the measurement setup chosen to correctly detect the horizontal and vertical behavior of the structure. Attention is especially focused on the excitation method, transducer selection (based on their metrological performances), the data acquisition system and the instrumentation placement.

Sensors choice is a crucial task to assure the needed quality of the acquired vibration signals. The sensors should be able to measure both low vibration levels, for example those due to environment excitation sources (wind, traffic, etc.), and higher levels, obtained by means of a forced excitation with a suitable actuator and, in the case of a permanent monitoring, by the operational loads on the structure (landing helicopter in this case). This requirement may be satisfied by transducers with a high sensitivity and consequently a low noise floor as evidenced by Cigada et al. in [16]. Furthermore, the transducer bandwidth must guarantee the acquisition of the all frequencies of interest. The main natural frequencies of interest are limited to the range 0.5–10 Hz. Taking into account all the above statements, the piezo accelerometers PCB 393B12 are chosen, which are characterized by a 0.1–500 Hz bandwidth, sensitivity 10 V/g, measurement range ±0.5 g and spectral noise 12.7 (μm/sec2)/$\sqrt{}$Hz in correspondence of 1 Hz. All the sensors are conditioned and acquired by means of a National Instruments device equipped with 24-bit acquisition modules with anti-aliasing filter. Thanks to the performances of the data acquisition system, a high sampling frequency is adopted, 2,048 Hz, and then data are digitally downsampled to obtain the final sampling frequency of 256 Hz. This way of sampling contributed to assuring an even higher signal to noise ratio in the measurement, which is a key feature when ambient vibrations are used.

As explained in the Sect. 2, the dynamic behavior is inspected both in horizontal and vertical directions. Moreover, the aim of this work is to compare the results obtained by applying both experimental modal analysis (EMA) and operational modal analysis (OMA). Consequently, the tests are performed, both in horizontal and vertical direction, with environmental excitation sources and with a proper forced excitation source, as explained in the following.

Planning a campaign on the basis of simulated data only is really difficult and risky due to a number of uncertain parameters, such as damping values that are not known and are meaningful in the choice of the forcing amplitude. For this reason, it is preferable to explore the structure response to environmental excitation with a preliminary test and

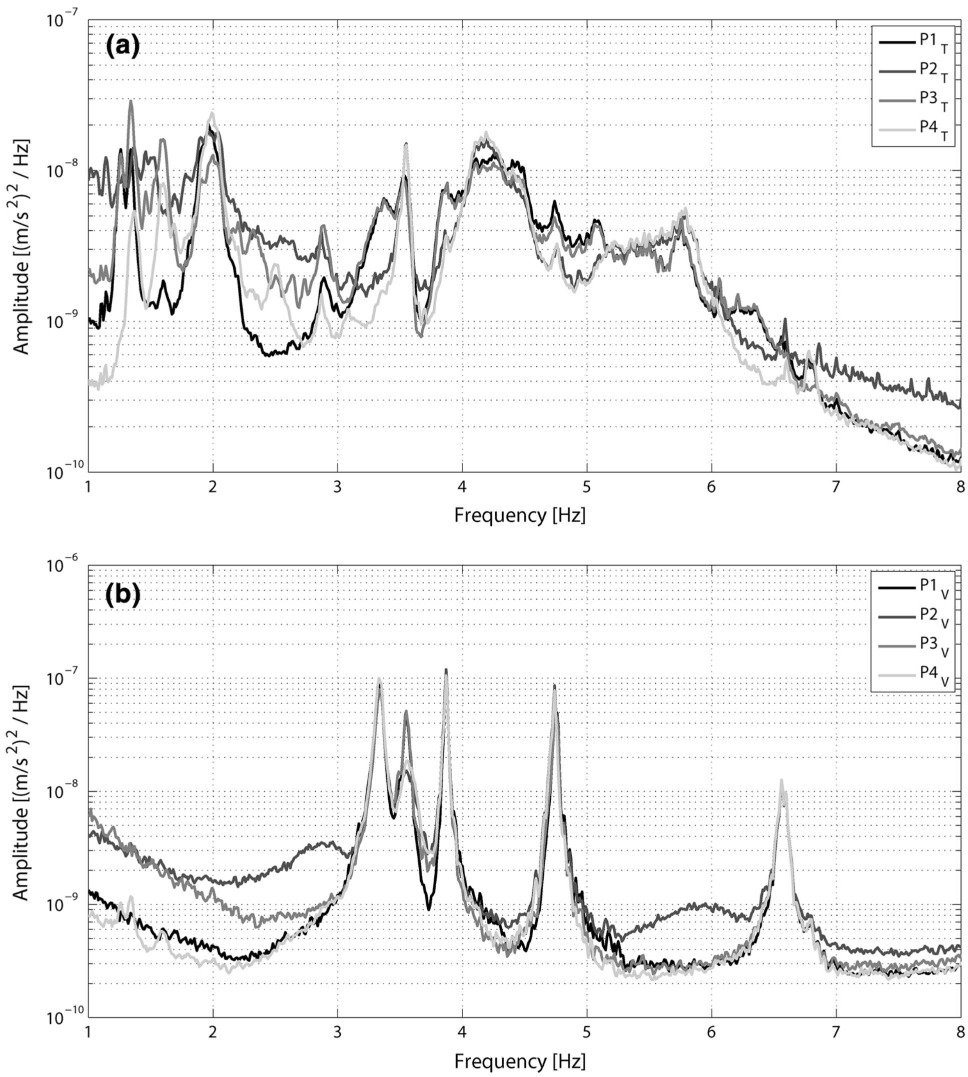

Fig. 4 PSD comparison between tangential accelerometers and vertical accelerometers

then use these data to design a proper measurement campaign. Assuming the helisurface to be a planar circle, four measurement points are placed at half radius of the circumference (position from 1 to 4 in Fig. 3). Every measurement point is composed of three accelerometers placed along the main directions: radial, tangential and vertical (gray arrows in Fig. 3) to estimate the main modes in all the directions as first approximation.

Figure 4 shows the power spectral densities of the four accelerometers placed along the tangential direction on the circular surface and the four accelerometers placed in the vertical direction. The results define two distinct behaviors of the structure. It has few high damped modes in the horizontal direction, which means that the forcing system must be able to introduce high energy into the structure to force these modes and obtain a measurable response. On the other hand, the vertical modes are less damped, making a common hydraulic actuator enough to force the structure in that direction, but, as more modes are involved, it is fundamental to improve the sensor number on the surface to estimate correctly all the mode shapes.

Moreover, as it will be explained in the following, the excitation in the vertical direction will be in different forcing points to distinguish the "double modes" always present in symmetrical structure, as in the considered helisurface.

In the following sections, two different measurement setups will be described for horizontal and vertical directions, respectively.

3.1 Horizontal direction

The adopted measurement setup in the horizontal direction is the same as shown in Fig. 3, both for EMA and OMA tests. The finite element simulation indeed reveals that the main modes in the planar directions are basically rigid body modes, due to the degree of freedom allowed by the multidirectional joints. The vertical accelerometers are used as well, since they may provide more information on pitch modes, which may be excited by the horizontal forcing sources.

EMA tests are carried out by forcing the structure with an inertial actuator. As shown in Fig. 4, the structure has a high damped behavior in the horizontal direction, which means that a huge amount of mechanical energy is necessary to sufficiently excite the modes in that direction. As the force is proportional to the mass and the acceleration, once the frequency of interest is fixed as a maximum of 10 Hz, the only two parameters left to design the forcing system are the mass and its stroke. As a huge mass with a short stroke would be difficult to manage (local load increase could damage the structure), the only reasonable possibility is a forcing system design with a long stroke and a lighter inertial mass. Among the traditional inertial actuators, a hydraulic system could be used, but its hydraulic devices would not be easily moved on the heli-surface. The solution to the problem is found in a linear permanent magnet motor produced by SIEMENS. It is considered the best way to excite the structure, as the available stroke is 2 m long and the system is designed to move an inertial mass of up to 1.5 tons, which is enough to introduce a meaningful amount of energy even at the

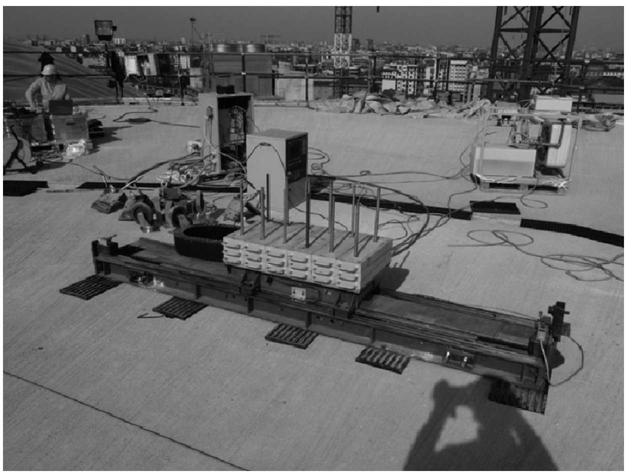

Fig. 5 Linear motor with slide and mass used as an actuator

Fig. 7 Hydraulic actuator and mass used

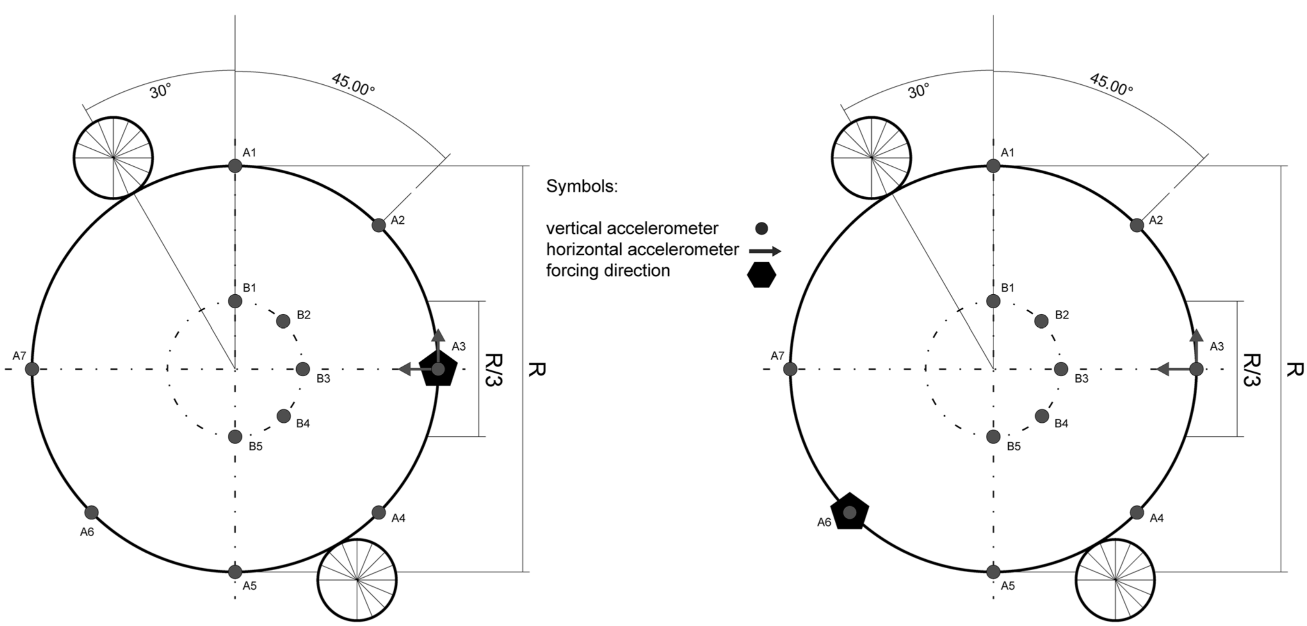

Fig. 6 Sensor placement for the vertical direction

lowest frequencies of interest (1 Hz). Figure 5 shows the actuator positioned on the surface and the sliding mass of 540 kg adopted during the tests.

The frequency response function of the structure is estimated by means of a stepped sine harmonic excitation: the covered frequency band is in the 0.1–10 Hz range with a resolution of 0.05 Hz in correspondence to the resonances and 0.1 Hz in the other frequency intervals. The system is actuated imposing constant acceleration amplitude and therefore a constant force amplitude. According to Fig. 3, the actuator is placed in position 5 (1/3 of the surface radius) acting along a tangential direction. Three accelerometers are placed on the floor, in correspondence to the motor, to measure the vibrations introduced into the structure along the three main directions (radial, tangential and vertical). Moreover, an accelerometer is placed on the sliding mass, along the excitation direction, to estimate the force transmitted to the structure.

Concerning the OMA tests, the duration is about 48 h long to guarantee a sufficient amount of data and a robust estimation of the helisurface response spectral functions. Indeed, the relative low excitation imposed by environment forcing sources makes a huge amount of data necessary to separate the useful information from the noise, which normally affects the acceleration signals.

The Sect. 3.2 describes the setup used for the measurement of the vertical vibrations.

3.2 Vertical direction

As explained in the Sects. 2, 3, 3.1, the structure is symmetric and therefore will show coupled modes in the vertical direction. The requirements for detecting all the modes and guaranteeing the unique identification of couple modes lead to define the measurement setup described in the following and to force the structure at least in two

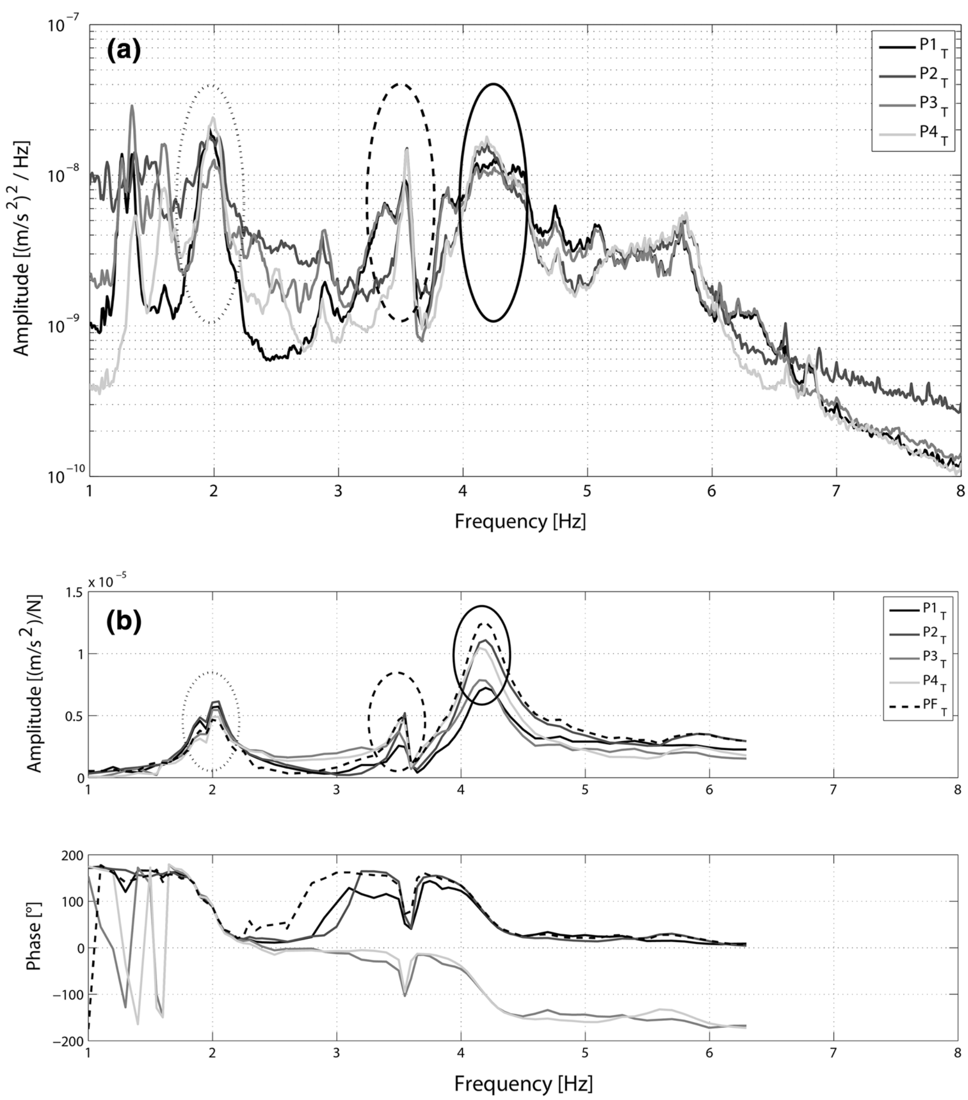

Fig. 8 **a** PSD tangential accelerometers. **b** FRF tangential accelerometers

different points. Figure 6 shows the sensor placement chosen for the vertical direction. In this case, the number of the measurement points increases up to 12, because the preliminary tests show that modes are more in number and with more complicated mode shapes.

Every measurement point is composed of one accelerometer placed along the vertical direction: seven accelerometers are located on the circumference (letter A in Fig. 6), whereas five accelerometers are placed on one-third of the radius (letter B in Fig. 6), inside the area of the constraints linking the platform to the main structure underneath. This measurement setup is chosen to detect the main vibration modes, conforming with the results obtained from the computer simulation, as for the horizontal tests. Like the horizontal direction, this measurement setup is the same for the EMA and OMA tests.

In this case, the forcing system is a hydraulic actuator placed in correspondence to point A3 and A6 of Fig. 6 to perform EMA tests. The need of two excitation points is given by the radial symmetry of the structure which requires more excitation positions to detect all the vibrations modes [9]. The actuator moves an inertial mass of 120 kg with maximum oscillation amplitude of 50 mm. The frequency response functions of the structure are estimated by means of a stepped sine harmonic excitation, covering the band between 2 and 10 Hz, imposing a frequency resolution of 0.05 Hz in correspondence to the resonances and 0.1 Hz otherwise. Unlike the horizontal forcing direction, the vertical displacement of the structure is more easily excitable with a smaller inertial mass and a shorter actuator stroke because the damping is low.

Operational modal analysis techniques are applied to the vertical measures to perform modal identification. As in the horizontal case, ambient vibrations are acquired continuously for 48 h.

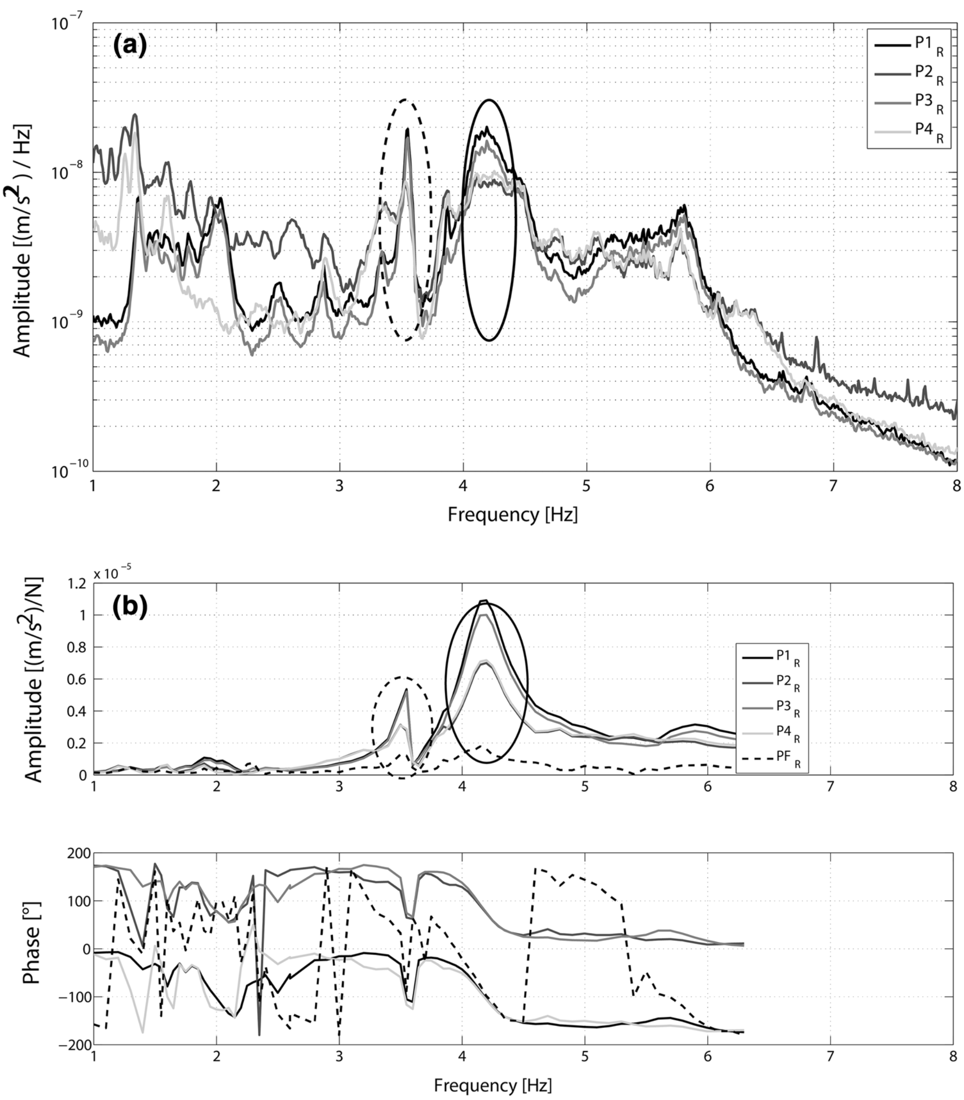

Fig. 9 **a** PSD radial accelerometers. **b** FRF radial accelerometers

Fig. 10 **a** PSD vertical accelerometers. **b** FRF vertical accelerometers

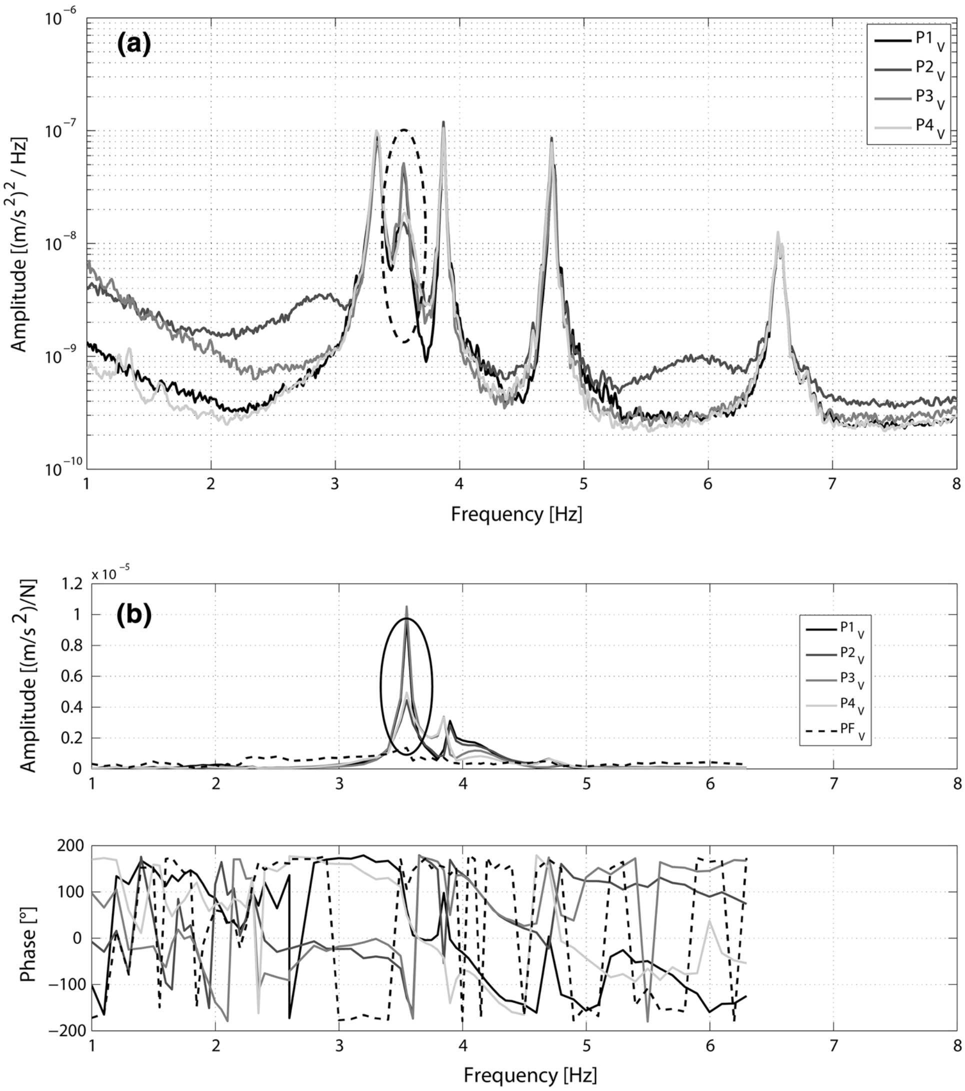

All the acquired data, both horizontally and vertically, are processed using the polyreference least square frequency domain method suitable for both OMA and EMA approaches [12, 17]. It must be noticed that the input of this method is the frequency response function (FRF) of the system. In the case of OMA tests, the method cannot be applied in a strict way, because the loading is not measurable. However, the same approach could be used if the loading is random and broad band enough. This algorithm is particularly suitable for highly damped structure, such as mixed concrete-steel ones. The obtained results are shown in the Sect. 4.

4 Results

In this section, the results obtained from EMA and OMA are presented, both for horizontal and vertical directions. At first, a comparison between the ambient vibration power spectral density and the experimental transfer function is shown, and then the identification results are compared. The first section describes the results coming from the horizontal measurement setup (Fig. 7).

4.1 Horizontal direction

In this section, the results from the horizontal measurement setup are discussed. Figure 8a shows the estimated power spectral density (PSD) of the tangential accelerometers (refer to Fig. 3 for the sensor position); three ellipses highlights the areas of main activity, even if it is clear that no predominant peaks are present. These three areas are confirmed by Fig. 8b, which shows the frequency response functions (FRF) obtained with the same measurement setup and forced conditions; three main peaks, circled with ellipses of the same line style used in Fig. 8a, are identified at frequencies compatible with the ones from operational data, which are less clear because the damping in the planar directions is high.

Table 1 Identified frequencies, damping values and modal residues

Mode	1 E	1 O	2 E	2 O	3 E	3 O
Frequency (Hz)	1.98	1.97	3.54	3.56	4.14	4.17
Damping (%rc)	5.26	4	0.7	1.2	3.81	3
Modal residues						
P1_R	0.14	−0.48	0.56	0.55	−0.89	−1.10
P1_T	−0.92	0.87	−0.28	0.45	0.54	1.00
P1_V	−0.05	0.16	−0.87	−0.98	−0.12	−0.46
P2_R	−0.09	0.60	−0.33	−0.45	0.54	0.83
P2_T	1.00	1.00	−0.53	−0.53	0.89	0.98
P2_V	0.03	−0.43	0.47	−0.75	0.13	0.63
P3_R	−0.11	0.50	−0.55	−0.47	0.82	1.00
P3_T	0.93	0.79	0.37	0.45	−0.61	−0.95
P3_V	−0.03	−0.32	1.00	1.00	−0.10	0.49
P4_R	0.09	−0.34	0.35	0.45	−0.55	−0.94
P4_T	0.81	1.00	0.48	0.50	−0.85	−1.22
P4_V	−0.01	0.22	−0.57	−0.82	0.09	−0.59
PF_R	−0.04		−0.12		−0.16	
PF_T	−0.73		−0.55		1.00	
PF_V	−0.04		0.12		−0.02	

A similar situation is shown by the radial acceleration PSDs. The ellipses in Fig. 9a highlight two areas of main activity, which are not strongly predominant with respect to other frequency bandwidths. However, they found correspondence in the FRF shown in Fig. 9b, where the two amplified peaks are well defined. Because the peak around 2 Hz is not shown in the radial accelerations, probably the corresponding mode shapes are referred to a rigid torsion in the horizontal plane allowed by the multidirectional joints.

Things change if the vertical acceleration PSDs are considered. Figure 10a show many clear peaks from 3 to 10 Hz. Among these, the peak around 3.5 Hz, observed both in the tangential and radial accelerations of Figs. 8a, 9a, is still present. However, the corresponding FRF practically shows only the peak around 3.5 Hz; see Fig. 10b. This peak, as it will be better explained in the Sect. 4.2, corresponds to a pitch motion along the forcing direction (mode with 1 nodal diameter). This mode has a shape that makes it excitable both with vertical and horizontal forcing, while the other peaks in the PSD correspond to modes that are excitable only by vertical forces and therefore disappear in the horizontal forcing FRFs. All these mode shapes will be described and investigated in the vertical forcing results section.

Both data sets, operational and experimental, show that the structure has principal modes in the vertical direction which are easily forced by environment excitation sources, since the PSDs along that direction show clear peaks with low damping. The planar modes are instead hardly forced by environment forcing sources because of the high structure damping and the multidirectional joint constraints. The comparison between the two sets of data is also described in terms of modal parameters estimation. Table 1 shows a summary of the three identified modes: it lists, for each mode, the frequency, the damping and the modal residues, obtained both from experimental and modal analyses. First of all, a good agreement may be

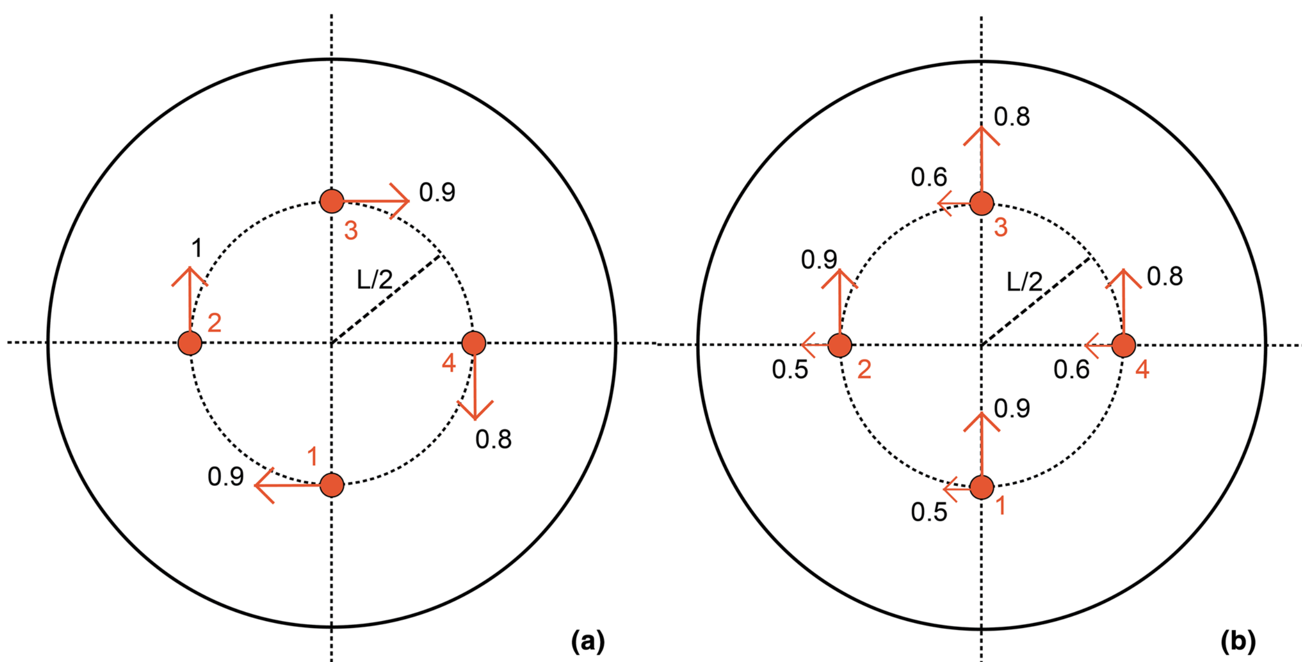

Fig. 11 **a** Mode shape for mode 1. **b** Mode shape for mode 3

Fig. 12 CMIF in horizontal direction

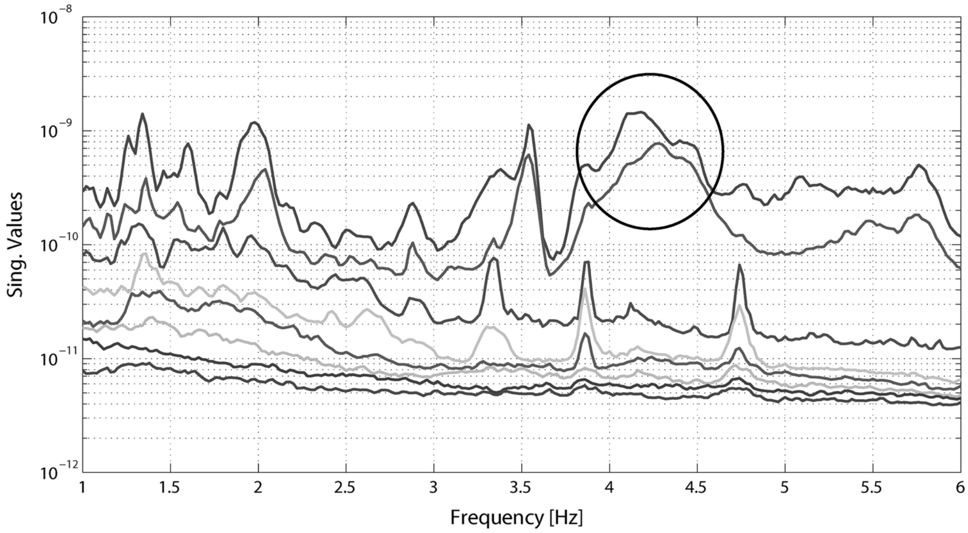

Fig. 13 **a** PSD vertical accelerometers. **b** FRF vertical forcing in A3

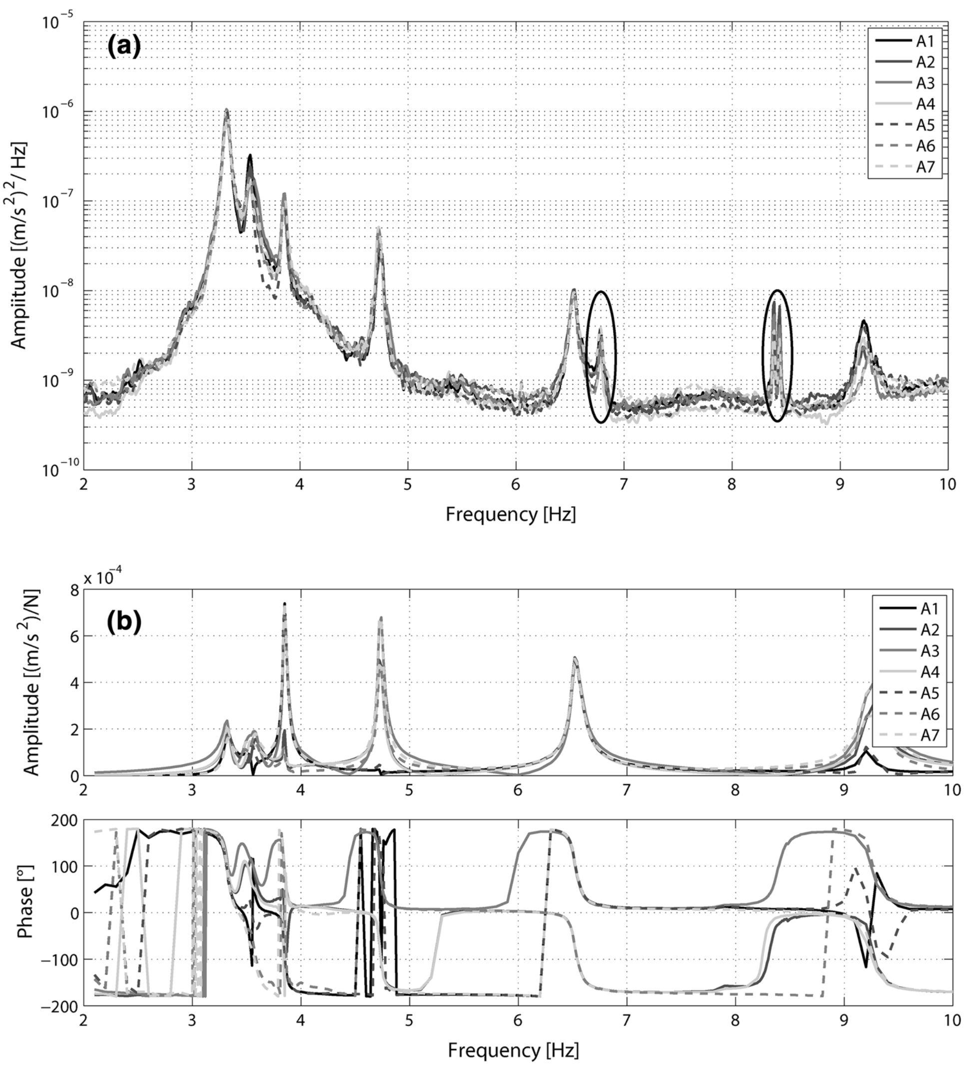

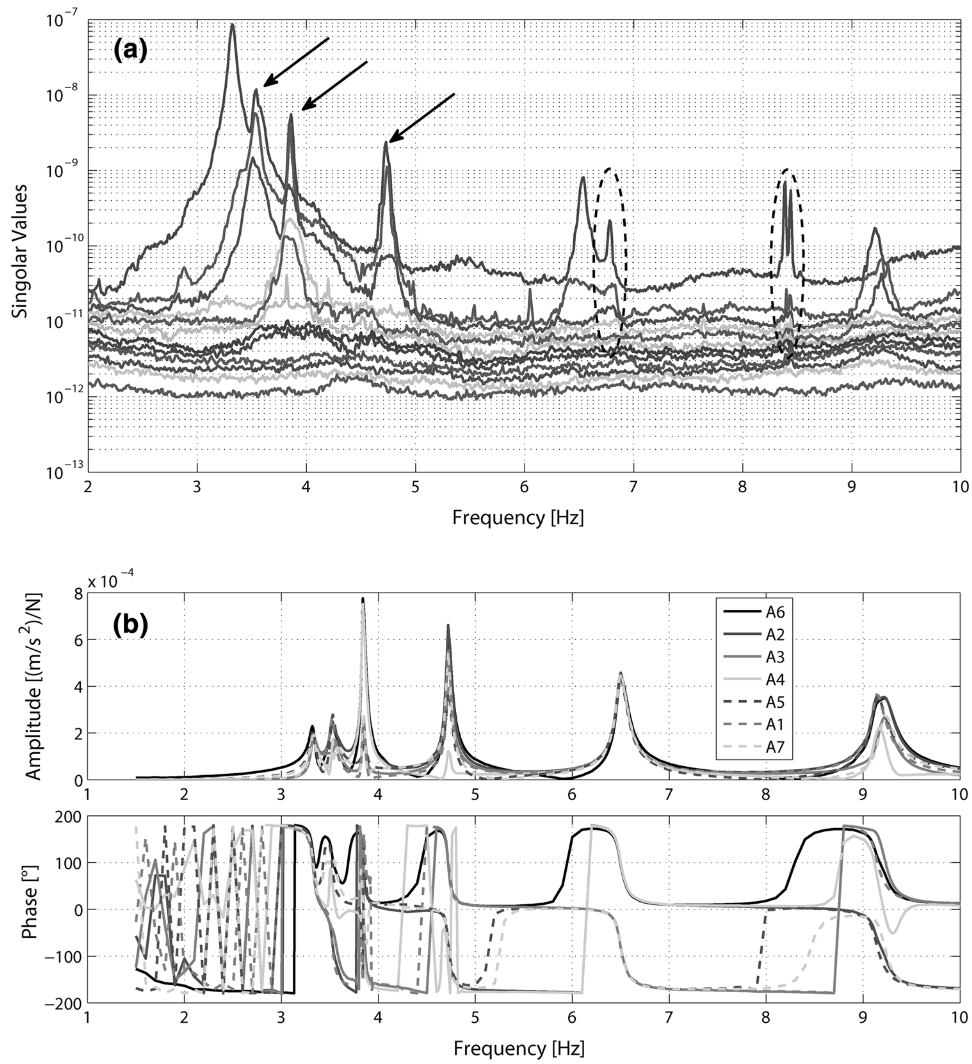

Fig. 14 **a** CMIF vertical direction. **b** FRF vertical forcing in A6

found in the frequency values, whereas the damping values show higher discrepancies between operational and experimental analyses. A difference in the damping values can be justified by the signal to noise ratio, which is surely better in the EMA tests than in the OMA ones, and by the different vibration amplitude reached in the EMA tests. A slightly nonlinear behavior in the damping values, normally increasing with vibration amplitudes, has to be expected in these kinds of structures where the effects of the internal friction are important. Moreover, it can be seen that the damping values along the horizontal direction are higher than the vertical ones, which is probably due to the hysteresis of the neoprene supports.

The identified mode shapes are basically the same, but it must be noticed the highest energy introduced during the EMA tests allows obtaining a better estimation of the modal residues. An example is mode 1 that is a rigid rotation of the planar surface around its axis (see Fig. 11). Experimental modal analysis results are clearer to explain, as the tangential measurement points all have values around one and the same phase, whereas the residues of the other directions are basically zero. Operational modal analysis results for the tangential directions are nearly the same, but, if the other directions are observed, the residues show not negligible values. The EMA practically gives a 0 value for all the residues, which is the correct value for this mode shape, while the OMA gives values higher than 0, due to the low vibration amplitudes. It must be noticed that the residue values are normalized to the maximum of each eigenvector, and so, if the vibration amplitude is very low (nearly at the same level as measurement noise), there may be a little difference in the residue values between different points. The same considerations about OMA results can be referred to mode 3 which is the next mode along the planar directions, whereas mode 2 (corresponding to 3.54 Hz), as stated below, is a pitch rigid body mode that will be described in the Sect. 4.2. These results reveal that OMA tests are characterized by a high level of uncertainty in terms of dynamic parameters estimation and, therefore, it may be difficult to use horizontal modes for health monitoring based on OMA.

The identified mode shapes, obtained by the EMA tests, for mode 1 and 3 are shown in Fig. 11. The first mode is the above-mentioned rigid rotation around the central axis, while the second is a rigid translation of the disc in the excitation direction. It has to be pointed out that mode 1 is clearly identified; the differences among the residues in the tangential direction can be ascribed to the estimation uncertainty since the residues in the other directions are nearly insignificant. Moreover, mode 3 displacement direction will always be in the forcing direction, as this is a double mode of the structure in the horizontal plane. As shown by the modal residues in Table 1, the modes obtained from OMA are unreliable without a comparison with those obtained by EMA tests, since the residues not involved in the mode shape (for example the radial residues in the first horizontal mode) are overestimated due to the bad signal to noise ratio. Looking at the CMIF (common mode indicator function) shown in Fig. 12, it can be seen that two singular values have a meaningful amplitude (even if signal to noise ratio is not favorable to the identification) stating that two vibration modes are co-existing at this frequency as well known from literature [12].

4.2 Vertical direction

As previously stated, EMA tests in the vertical directions are repeated twice, changing the forcing point to identify and distinguish all the "double" modes of this structure, which is practically axial symmetric also for the constraint conditions. Figure 13a, b shows the PSD and FRF obtained from the vertical accelerations. At a first glance, it can be seen the PSD obtained from the vertical vibrations show a higher number of peaks in the same frequency range, but some of them are not present in the FRF plot (gray circles in Fig. 13a). These are most likely due to harmonic excitation given by some activities occurring in the proximity of the helisurface that can be erroneously identified as vibration modes, if only the operational data are considered [18]. This drawback must be taken into account if structural health-monitoring techniques are to be applied, since they are mostly based on automatic data analysis to extract the damage features, which could lead to erroneous conclusions if the structures dynamic parameters are not clearly identified.

Figure 14 shows the common mode indicator function of the cross-spectral matrix, obtained from the environment vibration data, and the FRF response functions computed for the second forcing point (point A6 in Fig. 6b). Looking at the CMIF of Fig. 14, three peaks, indicated by black arrows, are characterized by two singular values having non-neglectable amplitude. Moreover, it can be seen that two spurious peaks circled by black eclipses are still present and there is a risk of the possibility of identifying them as structural modes [18]. The easiest way to discard these peaks is to look at the experimental data, where they totally disappear, as seen in Fig. 14b. Nevertheless, the common mode indicator function applied to operational data clearly identifies the double modes in the structure with only one measurement session. The forced tests can achieve the same results only by moving the excitation source in another point of the structure, as done in this work for comparison purposes, and then looking at the modal residues or applying the CMIF to the forced response matrix. However, this requires two different test session and is therefore time and money consuming [17, 19]. The need to compare OMA and EMA data sets at the beginning of the structure life appears clear with these results, since EMA results help to define the correct parameters useful to structural monitoring, dismissing the misleading and uncertain data.

As next step, the polyreference least square algorithm is applied to the experimental data and a resume of the identified modes is given in Table 2 in terms of frequencies damping and modal residues. The residues of measurement points B are negligible, since these points correspond to the joints of the structure. For this reason their use in terms of a future structural monitoring will be irrelevant.

The identified mode shapes (EMA tests) are clearer if their graphical representation is observed in Fig. 15. The arrow represents the modal residue measured in each point and the number is the normalized residue amplitude (normalized to the maximum of each eigenvector).

Table 2 Modes identified in the vertical direction

Mode	1	2	3	4	5	6
Frequency (Hz)	3.32	3.56	3.85	4.73	6.53	9.25
Damping (r/rc) (%)	1.00	1.20	0.40	0.40	0.65	0.60
Modal residues						
A1	0.96	−0.13	−1.00	−0.02	−1.00	−0.01
A2	0.93	0.58	−0.06	0.73	1.00	−0.71
A3	1.00	1.00	0.95	−0.99	−0.96	1.00
A4	0.92	0.64	−0.03	0.71	0.97	−0.66
A5	0.83	−0.17	−0.94	−0.04	−0.97	−0.04
A6	0.83	−0.78	0.04	−0.70	0.99	0.66
A7	0.90	−0.92	1.00	1.00	−1.00	−0.98
B1	0.01	−0.01	−0.03	0.00	−0.02	0.00
B2	0.02	0.02	0.00	0.02	0.02	−0.01
B3	0.02	0.03	0.02	−0.02	−0.01	0.01
B4	0.02	0.03	0.00	0.02	0.02	−0.01
B5	0.02	−0.01	−0.03	0.00	−0.02	0.00
A3R	−0.06	−0.15	−0.04	0.07	0.07	−0.07
A3T	−0.04	−0.04	−0.04	0.01	0.01	−0.01

The same results, with the obvious phase shifts in the mode shapes, have been found for the second forcing point and similar results are obtained from operational data. In the latter case, particular attention has to be paid to the double modes because treating them as simple modes may lead to erroneous identification of the residue values. As an example, Table 3 shows the modal residue values identified in correspondence to the first two modes, which are well described by the space resolution of the adopted measurement setup, for the three tests:

- EMA A3: Forced testing, forcing in A3
- EMA A6: Forced testing, forcing in A6
- OMA: Ambient vibration testing

Looking at the results shown in Table 3, it can be seen that the agreement between the results is optimum for the first considered mode, which is a "single" mode. In this case the frequency value is practically the same, damping is similar and the modal residues are the same. However, mode 2 is coupled and shows more difference in the identified frequency and damping values. Moreover, the modal residues identified via EMA techniques, the ones identified by EMA forced in point A3 and EMA forced in point A6, seem different but refer to the same mode shapes (1 nodal diameter), shifted in space according to the forcing position; whereas the modal residues identified via operational modal analysis, under the hypothesis that one mode is present, are

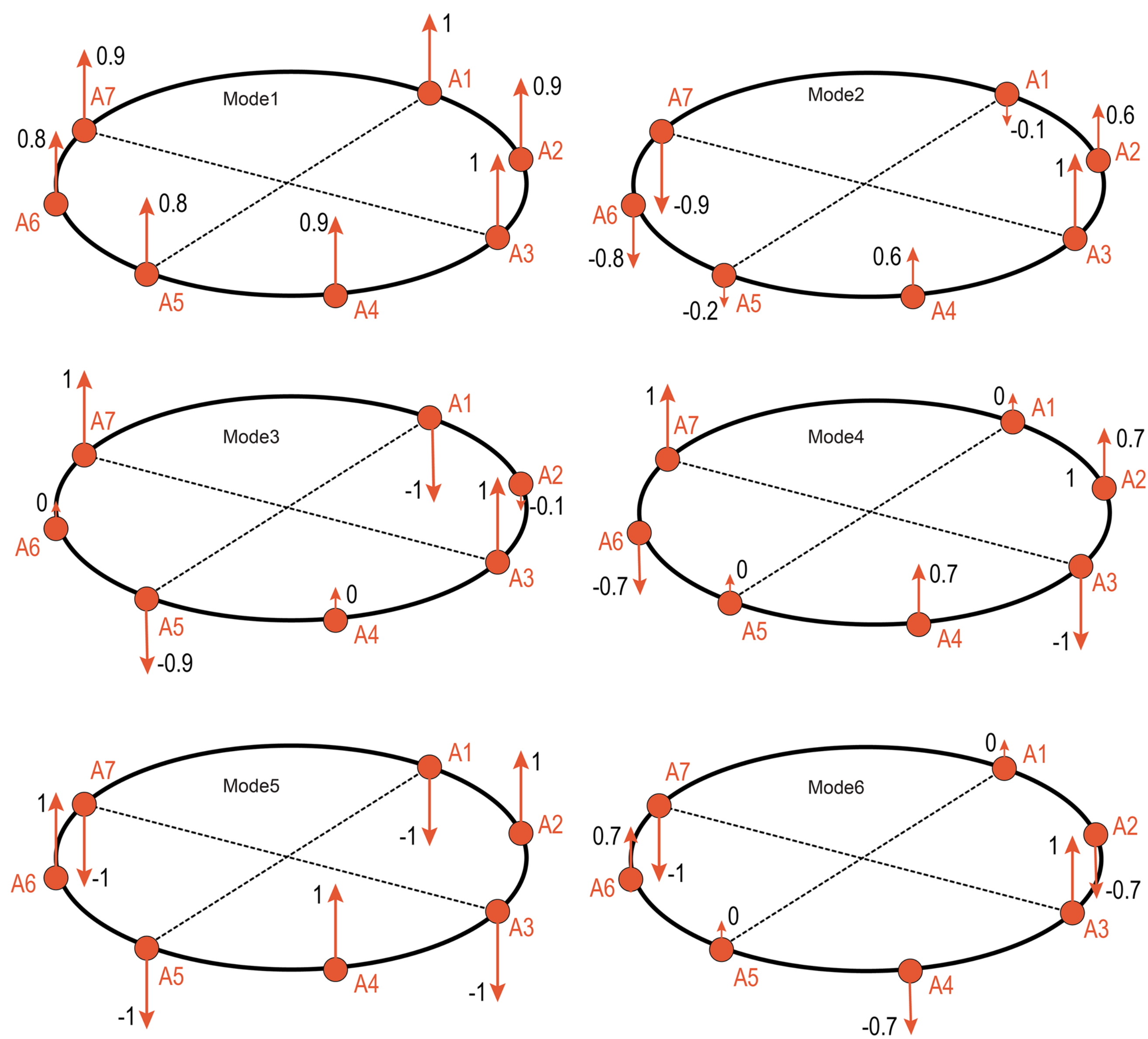

Fig. 15 Identified mode shapes forcing in A3

Table 3 Comparison between the first two identified modes for three different tests

Mode	1 EMA A3	1 EMA A6	1 OMA	2 EMA A3	2 EMA A6	2 OMA
Frequency (Hz)	3.32	3.33	3.32	3.56	3.53	3.54
Damping (r/rc) %	1.0	0.9	1	1.2	0.9	0.9
Modal residues						
A1	0.96	0.94	1.00	−0.13	0.87	1.00
A2	0.93	0.87	1.04	0.58	1.00	0.90
A3	1.00	−0.86	1.06	1.00	0.64	0.79
A4	0.92	−0.87	1.03	0.64	0.32	−0.75
A5	0.83	1.00	1.03	−0.17	−0.98	−0.85
A6	0.83	0.99	0.97	−0.78	−0.99	−0.80

misleading. The values are similar at all points, while phases are sometimes 0° and sometimes 180°. In this case, a deeper analysis has to be carried out taking into account the presence of two modes at approximately the same frequency. Operational modal analysis shows drawback in the identification of parameters corresponding to coupled modes of this structure and will the troublesome for its application to structural health monitoring. It must be stressed that the problem is not the identification method, but the noise to ratio value which is untoward in this specific structure, since PolyMax algorithm is known to be able to identify double modes [20, 21].

In the end, Fig. 14 show the common mode indicator function of the cross-spectral matrix, obtained from the ambient vibration data, and the FRF response functions computed for the second forcing point. In Fig. 14a, two peaks (underlined with gray circles) appear in the ambient vibrations, but do not correspond to any evident structural modes defined in the experimental modal analysis. Further analysis is considered necessary to improve the knowledge about this phenomenon. A time–frequency transform is

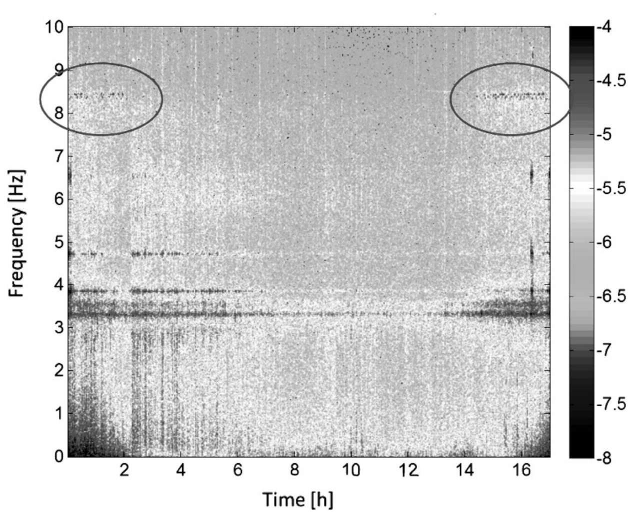

Fig. 16 Time frequency diagram of a vertical acceleration during 17 h

performed on a 17 h period data and the results are shown in Fig. 16. In the diagram on the x-axis is time, on the y-axis are the frequencies, and the colors are proportional to acceleration amplitude according to the scale on the left.

The two circled area in Fig. 16 are in correspondence to the peaks around 8.2 Hz, but the same conclusion may be drawn for that around 6.5 Hz. As it can be seen, they are not continuously present in the diagram, appearing only at the beginning and at the end of it. On the other hand, continuous lines of high amplitudes are present through the entire diagram in correspondence to the main structural resonances. From this diagram we may conclude that frequencies around 8.2 and 6.5 Hz are not from any resonance, but probably produced by some kind of force appearing or disappearing depending on the time of the day, probably due to some nearby constructions.

5 Conclusion

This paper studies the application of modal analysis theory to the investigation of the main vibration modes of the helicopter landing surface of the "Nuova sede Regione Lombardia" building. Two kinds of testing have been adopted, one exploiting experimental modal analysis techniques, and therefore applying a known loading to the structure, and the other exploiting natural ambient vibrations and operational modal analysis techniques. Tests have been carried out both along the horizontal and vertical directions. A particularly effective horizontal forcing system has been employed, allowing to provide enough energy input even at low frequencies, exploiting the unique features of a long stroke linear motor. The system proved to be suitable even for a highly damped structure like the tested one.

The main structural modes have been clearly identified and a comparison between experimental and operational results has been shown. It has been highlighted that EMA results are useful to fully understand the operational analysis ones, particularly when a low signal to noise ratio is experienced during the OMA tests. In some of the considered modes, the lack of energy led to an uncertain mode shape identification in the OMA tests, while some frequencies present in the signal power spectral densities were shown to be results of external forces and not part of the structure response. It remains clear that OMA offers the possibility of performing a fast and reliable analysis without the need of an applied external load and is therefore suitable for the long-term health monitoring of the structure, once its results are clearly interpreted.

References

1. Brownjohn JMW (2007) Structural health monitoring of civil infrastructure. Philos Trans A Math Phys Eng Sci 365(1851): 589–622
2. Doebling SW, Farrar CR, Prime MB (1996) Damage identification and health monitoring of structural and mechanical systems from changes in their vibration characteristics: a literature review". Los Alamos National Laboratory report LA-13070-MS
3. Sohn H, Farrar CR, Hemez F, Czarnecki J (2002) A review of structural health monitoring literature 1996–2001, in third world conference on structural control, pp 1–7
4. Doebling SW, Farrar CR, Prime MB (1998) A summary review of vibration-based damage identification methods. Shock Vib Dig 30(2):91–105
5. Carden EP (2004) Vibration based condition monitoring: a Review. Struct Heal Monit 3(4):355–377
6. Fan W, Qiao P (2010) Vibration-based damage identification methods: a review and comparative study. Struct Heal Monit 10(1):83–111
7. Reynolds P, Pavic A, Carr J (2007) Experimental dynamic analysis of the Kingston communications stadium. Struct Eng 85(8):33–39
8. Peeters B, De Roeck G (2001) Stochastic system identification for operational modal analysis: a review. J Dyn Syst Meas Control 123(4):659
9. Cigada A, Manzoni S, Vanali M (2008) Vibro-acoustic characterization of railway wheels. Appl Acoust 69(6):530–545
10. Ewins DJ (2000) Modal testing: theory, practice and application (mechanical engineering research studies: engineering dynamics series). Wiley, Hoboken
11. Caprioli A, Cigada A (2006) Comparison between different operational modal analysis techniques for the identification of large civil structure modal parameters. In: Proceedings of modal analysis of conference
12. Cornwell P, Farrar CR, Doebling SW, Sohn H (1999) Environmental variability of modal properties. Exp Tech 23(6):45–48
13. Mohanty P, Rixen DJ (2004) Operational modal analysis in the presence of harmonic excitation. J Sound Vib 270(1–2):93–109
14. Huth O, Feltrin G, Maeck J, Kilic N, Motavalli M (2005) Damage identification using modal data: experiences on a prestressed concrete bridge. J Struct Eng 131(12):1898
15. Cigada A, Caprioli A, Redaelli M, Vanali M (2008) Vibration testing at Meazza stadium: reliability of operational modal analysis to health monitoring purposes. J Perform Constr Facil 22(4):228
16. Cigada A, Moschioni G, Vanali M, Caprioli A (2010) The measurement network of the San Siro Meazza Stadium in Milan: origin and implementation of a new data acquisition strategy for structural health monitoring. Exp Tech 34(1):70–81
17. Bart P, Van der Herman A, Patrick G (2004) The PolyMAX frequency-domain method: a new standard for modal parameter estimation? Shock Vib 11(3–4):395–409
18. Farrar CR, James GH III (1997) System identification from ambient vibration measurements on a bridge. J Sound Vib 205(1):1–18
19. Brincker R, Zhang L, Andersen P (2001) Modal identification of output-only systems using frequency domain decomposition. Smart Mater Struct 10(3):441–445
20. Peeters B, Patrick G, Van der Herman A, Bart C, Peter V (2004) Automotive and aerospace applications of the PolyMAX modal parameter estimation method. In: Proceedings of IMAC-XXII conference and exposition on structural dynamics
21. Peeters B, Lowet G, der Herman VA, Jan L (2004) A new procedure for modal parameter estimation. Sound Vib 38(1):24–29